Supplemental data

Extended Figure 1: Characterization of P84 and MY1-mG1 anti-mouse SIRPα mAbs

(**A**) Characterization of P84 anti-SIRPα allosteric antagonist mAb and (**B**) MY1-mG1 anti-SIRPα orthosteric antagonist mAb. *Upper left*: ELISA binding to SIRPα. *Bottom left*: Antagonist ELISA assay with SIRPα immobilized to plastic and revelation of the binding of murine CD47-hFc. *Upper right*: mouse macrophages and dendritic cells differentiated from bone marrow cells with 100ng/mL M-CSF or 20ng/mL GM-CSF respectively for 5 days were incubated for 1 hours on mouse CD47-Fc coated plastic ± anti-SIRPα mAbs. SIRPα protein was co-immunoprecipitated with the anti-SIRPα mAbs and its tyrosine phosphorylation was detected by western blot. *Bottom right*: schematic representation of the binding epitope of each anti-SIRPα mAbs.

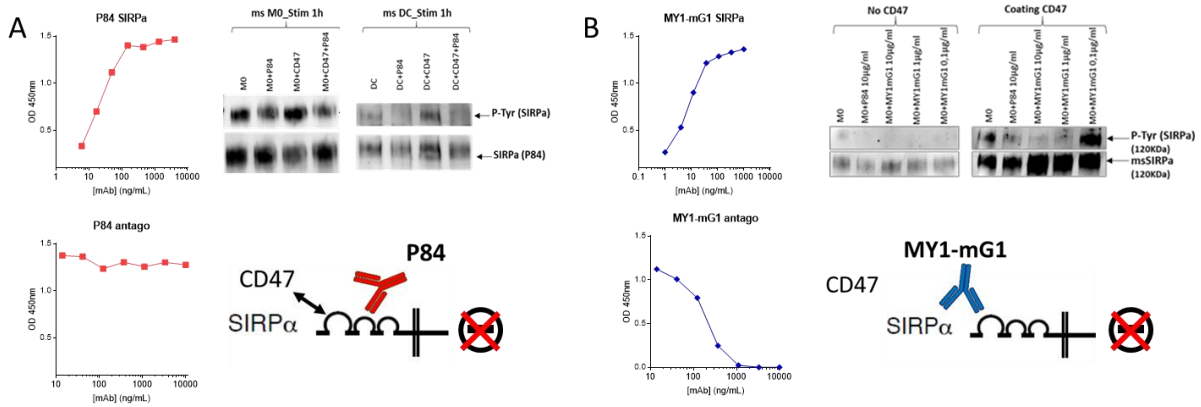

Extended Figure 2: Gating strategy and leukocytes quantification in the 4T1-mammary cancer orthotopic model microenvironment analysis (d10)

(*Top*) Gating strategy of one representative enzymatically-digested tumor for each treated group (control mouse compared to αSIRPα-treated mouse) analyzed by flow cytometry to identify macrophages (CD11b+/MHC-II+), M1-MΦ (CCR7+/CD206-), M2-MΦ (CCR7int/CD206+), NK cells (CD3-/NKp46+), or Treg (CD25+/CD127-) in CD4 T cells. (*Bottom*) Absolute counts of main leukocytes among live cells.

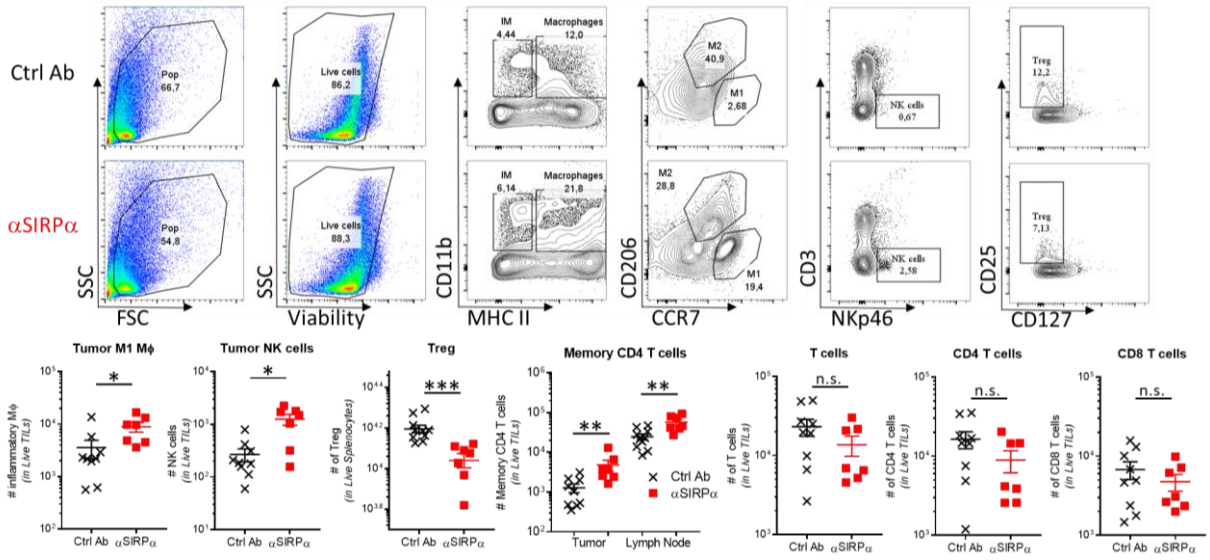

Extended Figure 3: SIRPα/CD47/PD-L1 expression by murine tumor cell lines

Flow cytometry phenotype of Hepa 1.6, MC38, AK-7 and 4T1 mouse tumor cell lines cultured 24 hours with or without 70 µg/ml of murine recombinant IFNγ.

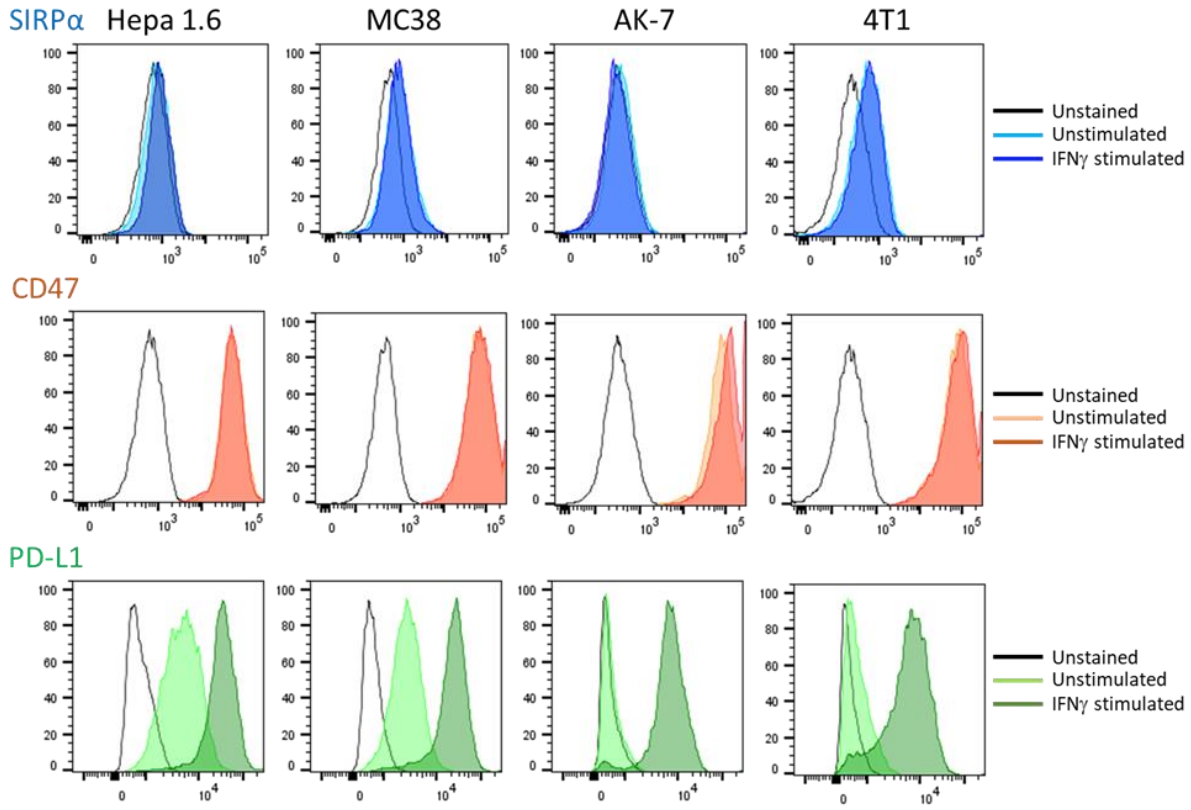

Extended Figure 4: Anti-SIRPα MY1-mG1 treatment in monotherapy and combination with anti-PDL1 and 4-1BB mAbs in the orthotopic hepatocellular carcinoma mouse model

(**A**) Survival of mice injected with Hepa 1.6 HCC cells ($2.5.10^6$) through the portal vein of C57Bl/6 male mice, and then treated from d4 to d28 with control Ab or anti-SIRPα (MY1-mG1) three times a week at 10mg/kg, or/and anti-PD-L1 twice a week at 6mg/kg. (**B**) Same as in (A) with anti-4-1BB mAbs treatment in monotherapy or MY1-mG1 combination injected injected twice at 3mg/kg on day 4 & 8 days after tumor injection. (**C**) Survival of tumor-free SIRPα+4-1BB-treated mice and rechallenged with $2.5.10^6$ Hepa 1.6 cells into the spleen 2 months after complete rejection. $^{**}P < 0.01$ (Log-rank test)

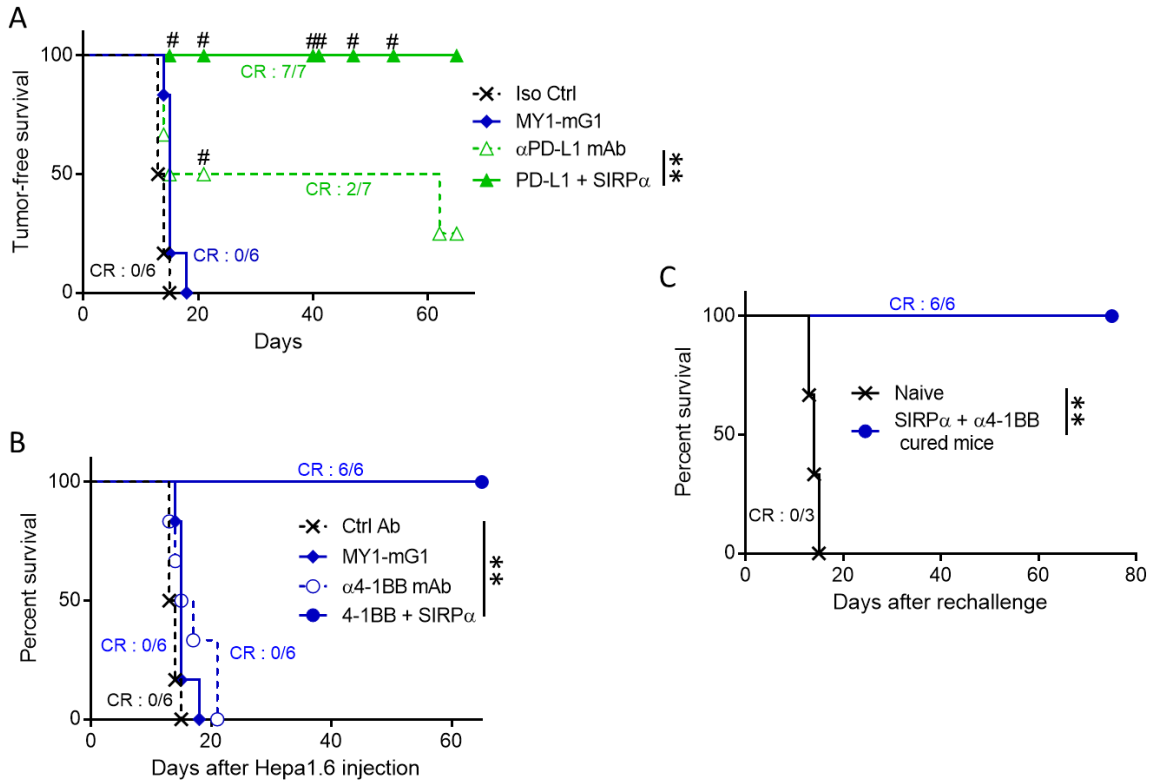

Extended Figure 5: Impact of SIRPα genetic deficiency alone or in combination with 4-1BB agonist in the orthotopic hepatocellular carcinoma mouse model

(**A**) Survival of mice injected with Hepa 1.6 HCC cells ($2.5.10^6$) through the portal vein of WT or SIRPα mutant C57Bl/6 mice treated or not twice (3 mg/kg on day 4 and 8) with anti-4-1BB mAbs. (**B**) Survival of tumor-free SIRPα mutant mice treated initially with the 4-1BB agonist and rechallenged with $2.5.10^6$ Hepa 1.6 cells into the spleen 2 months after complete rejection. (**C**) Survival of untreated mice after adoptive transfer of $2.5.10^6$ isolated T-cells from splenocytes of cured SIRPα mutant mice treated with 4-1BB and challenged with $2.5.10^6$ Hepa 1.6 cells in the portal vein the same day. $^{**}P < 0.01$ (Log-rank test)

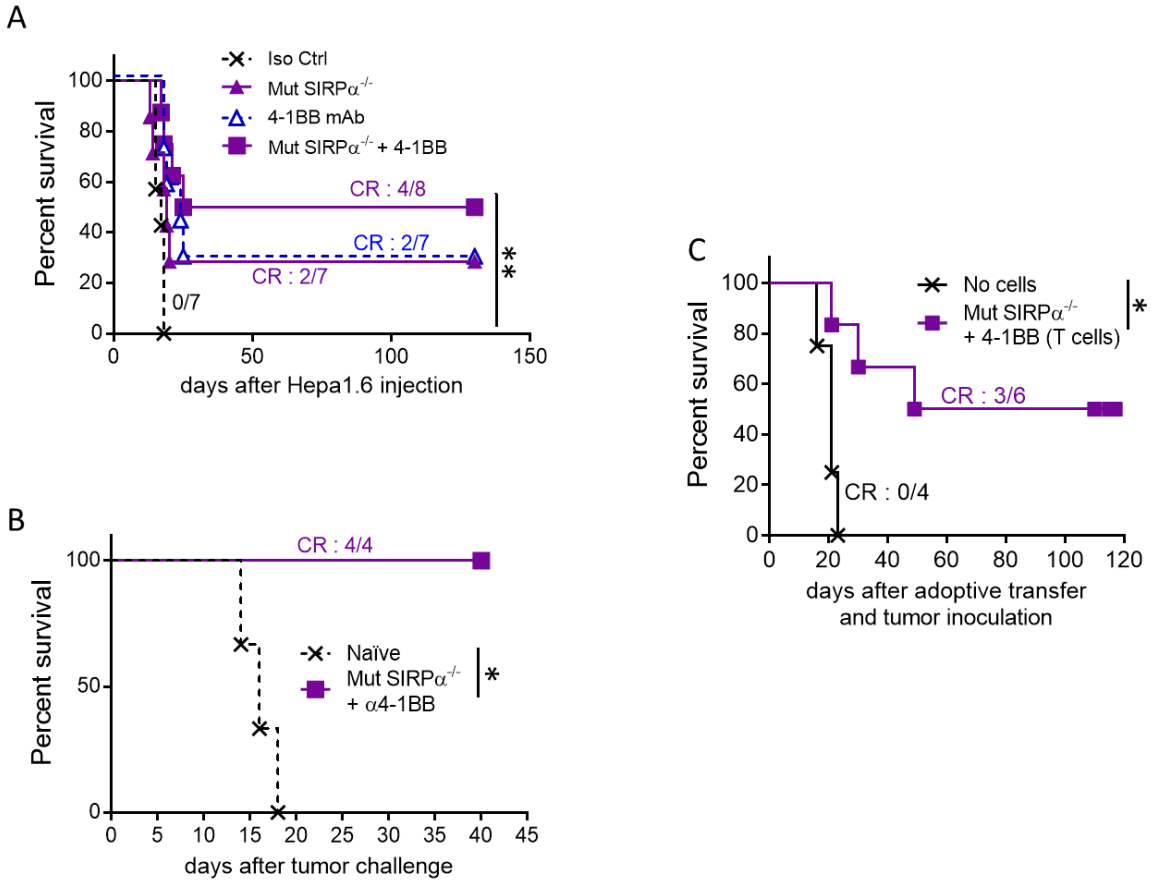

Extended Figure 6: Characterization of adaptive immune responses against Hepa 1.6 cells.

(**A**) Splenocytes isolated from cured mice in the Hepa1.6 model after treatment with anti-SIRPα+PD-L1 were cultured for 5 days with different irradiated mouse tumor cell lines (5 splenocytes for 1 tumor cell ratio). The proliferation was determined by H^3-thymidine incorporation to determine the specificity of memory T cells generated *in vivo* towards Hepa1.6 antigens. Peripheral plasma from Hepa 1.6-bearing mice were collected after ten days of treatment and tested for the binding on Hepa 1.6 cells (**B**) or normal hepatocytes (**C**) by flow cytometry and ELISA. **P* < 0.05, ***P* < 0.01 (unpaired Mann-Withney)

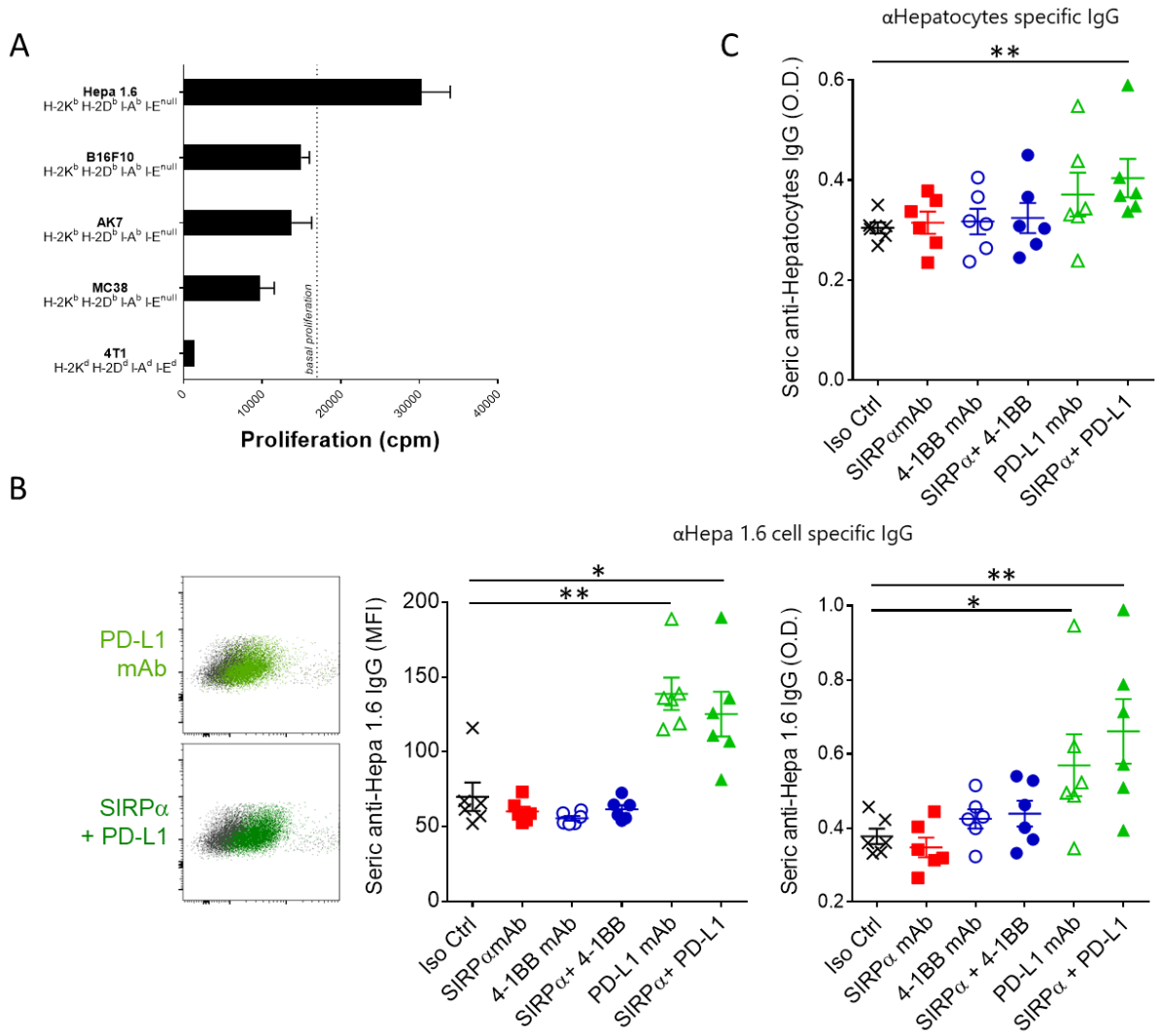

Extended Figure 7: Gating strategy of Hepa1.6-hepatocellular carcinoma orthotopic model tumor microenvironment analysis (d13)

Gating strategy of representative enzymatically-digested tumor analyzed by flow cytometry to identify macrophages (CD11b+/MHC-II+), M1-MΦ (CCR7+/CD206-), M2-MΦ (CCR7int/CD206+), Mo-MDSC (Ly6C+/Ly6G-) & PMN-MDSC (Ly6G+/Ly6Cint) among CD11b+/MHC-II- cells, CD4 T cells (CD3+/CD4+), CD8 T cells (CD3+/CD8+), NK cells (CD3-/NK1.1+), Treg (CD25+/CD127-) in CD4 T cells, B cells (CD19+) and the different subsets of B cells according their CD24/CD38 expression markers.

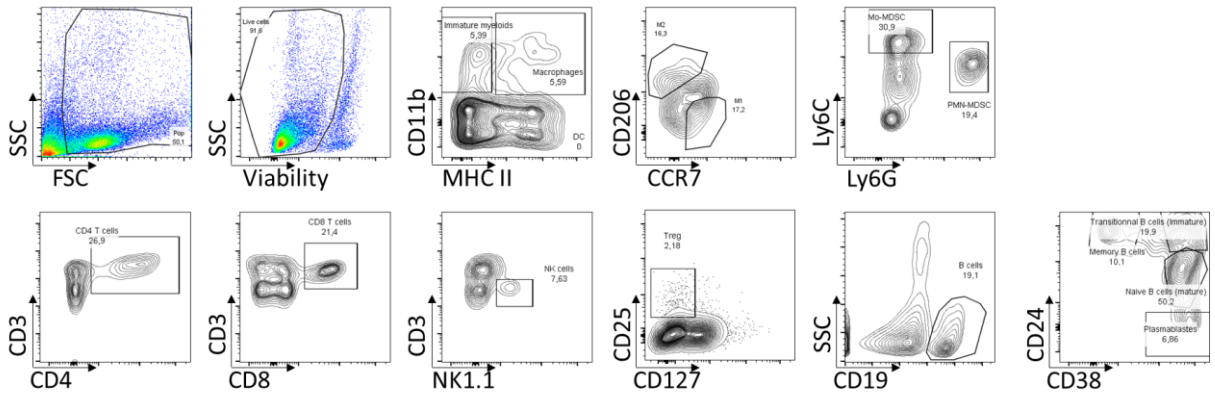

Extended Figure 8: Tumor infiltrating leukocytes modification after treatment in the orthotopic hepatocellular carcinoma model

Tumor infiltrating leukocytes, by excluding parenchymal cells from liver cell suspension, of Hepa 1.6-bearing mice were isolated after 10 days of treatment and analyzed by flow cytometry. *$P < 0.05$, **$P < 0.01$ (unpaired Mann-Withney or Kruskall-Wallis)

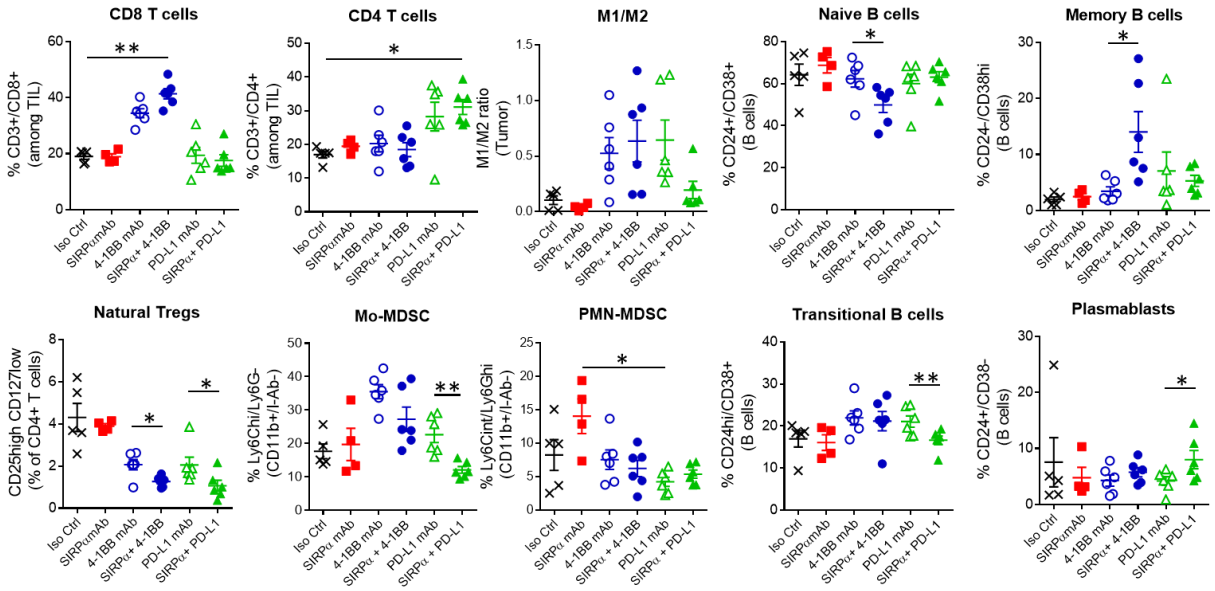

Extended Figure 9: Absolute counts of tumor infiltrating leukocytes modification after treatment in the orthotopic hepatocellular carcinoma model

Absolute counts among non-parenchymal cells (excluding tumor and parenchymal cells) for tumor infiltrating leukocytes of Hepa 1.6-bearing mice were isolated 13 days after tumor inoculation and analyzed by flow cytometry. *$P < 0.05$, **$P < 0.01$ (unpaired Mann-Withney or Kruskall-Wallis)

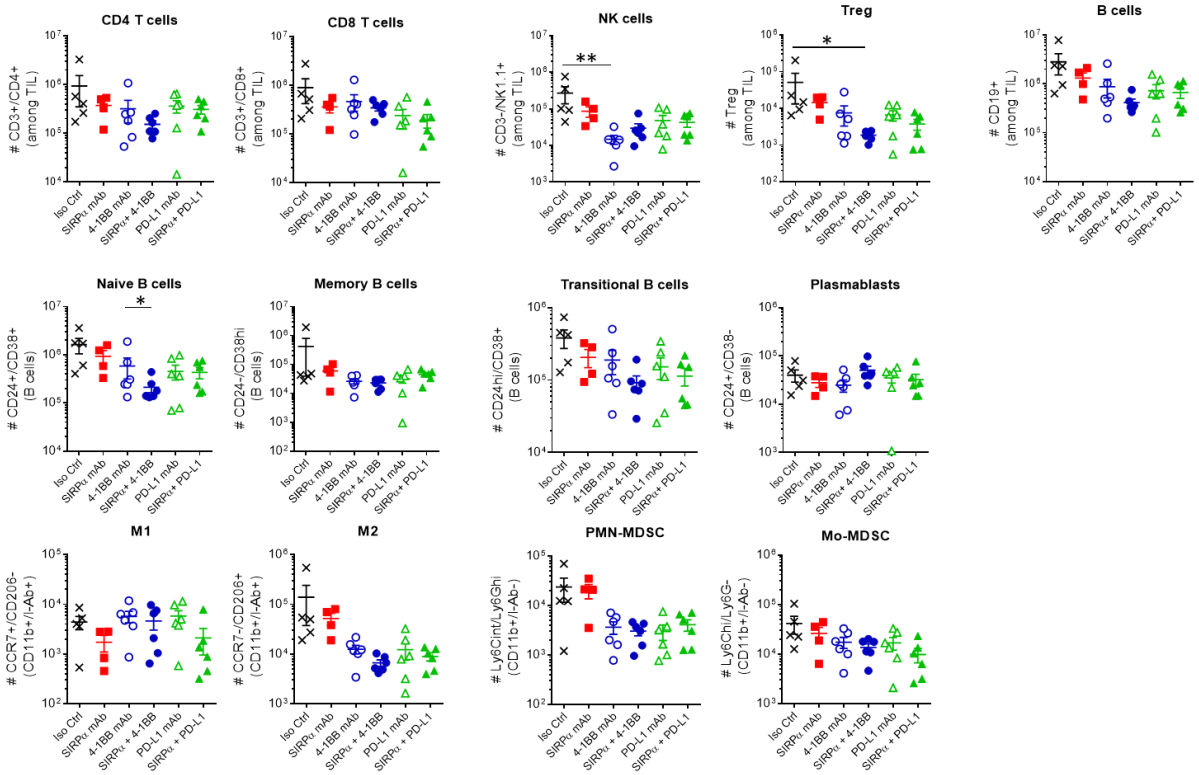

Extended Figure 10: Further tumor microenvironment transcriptomic modifications after anti-SIRPα combination therapy in mouse hepa1.6 model: pre-defined signature

Further transcriptomic Nanostring (PanCancer Immune Profiling panel) analysis, completing Figure 3, of the liver of mice in the orthotopic Hepa1.6 hepatocellular carcinoma model ten days after treatment initiation. Analysis of pre-defined Nanostring gene expression signatures of the following groups control mAb (black, n=6), P84 (red, n=6), anti-4-1BB alone (blue empty circles, n=6) or combined with P84 (blue plain circles, n=6), anti-PD-L1 alone (green empty triangles, n=6) or combined with P84 (green plain triangles, n=6). *$P < 0.05$, **$P < 0.01$ (unpaired Mann-Withney or Kruskall-Wallis)

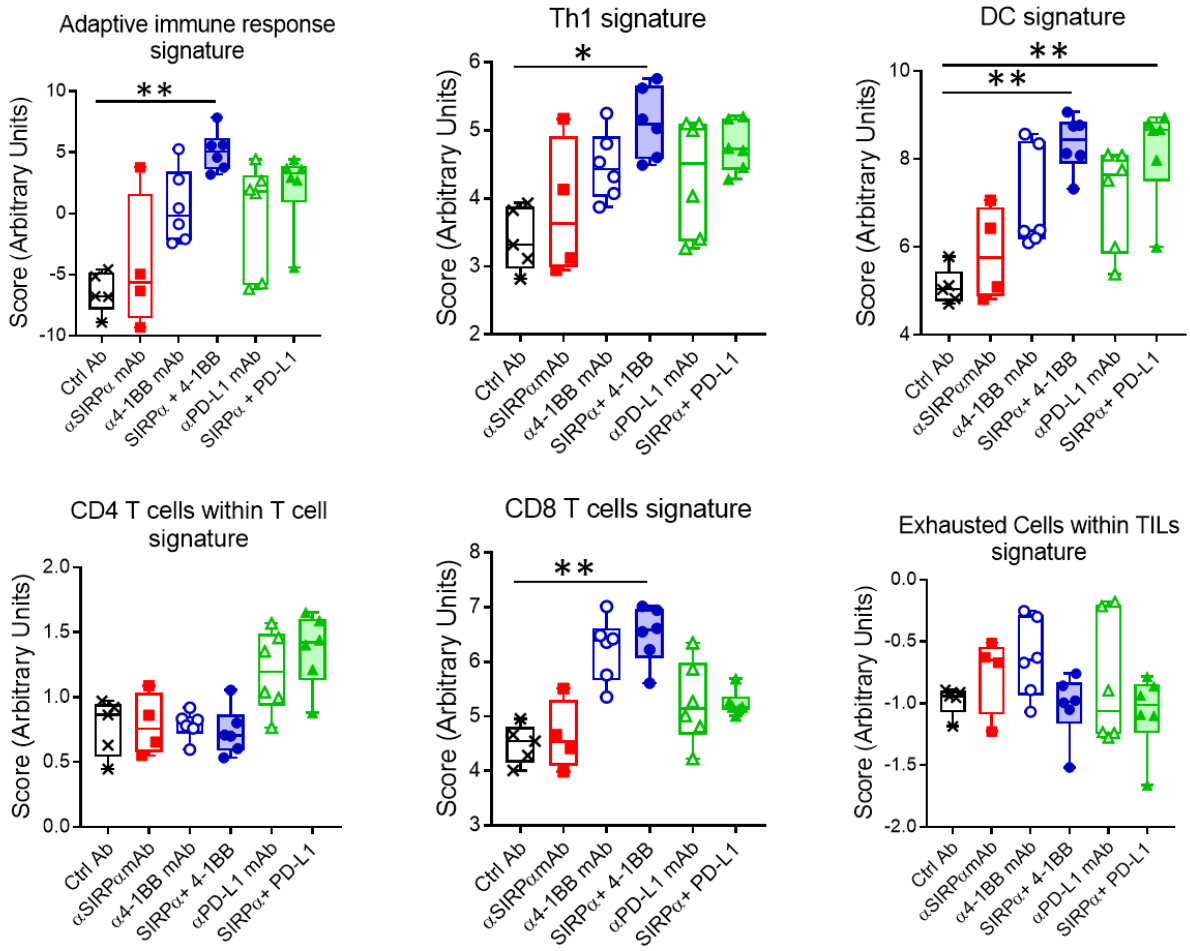

Extended Figure 11: Further tumor microenvironment transcriptomic modifications after anti-SIRPα combination therapy in mouse hepa1.6 model: PCA and downregulated genes

(**A-B**) Principal component analysis (PCA) of liver mRNA from Hepa 1.6-bearing mice performed with FaDA online software. Control group in red (N=5), anti-SIRPα in blue (N=4), anti-4-1BB or anti-PD-L1 in green (N=6 each), and anti-SIRPα combined with anti-4-1BB or anti-PD-L1 (N=6 each) in purple are depicted. (**C-D**) Genes listed and function relationship networks using the STRING tool representation of the downregulated genes cluster identified by a dotted line rectangle on heatmap on Figure 3. Genes related to TGFβ pathway and metastasis spreading are surrounded with black circle.

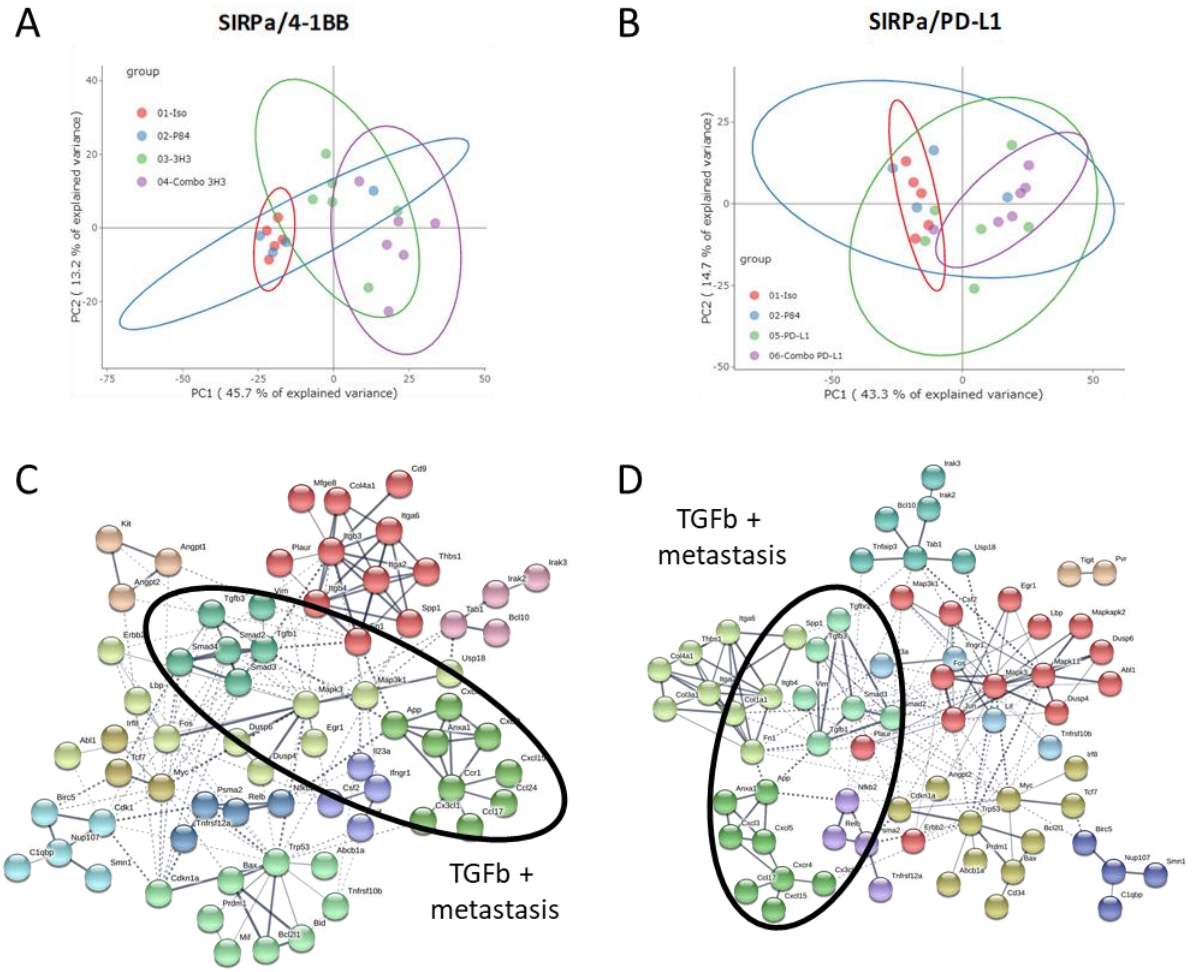

Extended Figure 12: <u>The selective anti-human SIRPα mAb (OSE-172) preferentially binds the V1 variant of hSIRPα</u>

(**A**) Characterization of anti-SIRPα mAb (OSE-172) binding on the two mains human SIRPα variants V1 and V2 by flow cytometry on blood monocytes from healthy volunteers. Representative histograms, dot plot, and graph of SIRPα expression on V1/V1 homozygous (green, N=8), V1/V2 heterozygous (blue, N=16), and V2/V2 (red, N=8) are represented. (**B**) Antagonist flow cytometry assay with αSIRPα mAb (OSE-172) on V1 and/or V2 SIRPα expressing monocytes and revelation of the binding of human CD47-hFc represented by the percentage of CD47-hFc binding in presence of the anti-SIRPα mAb.

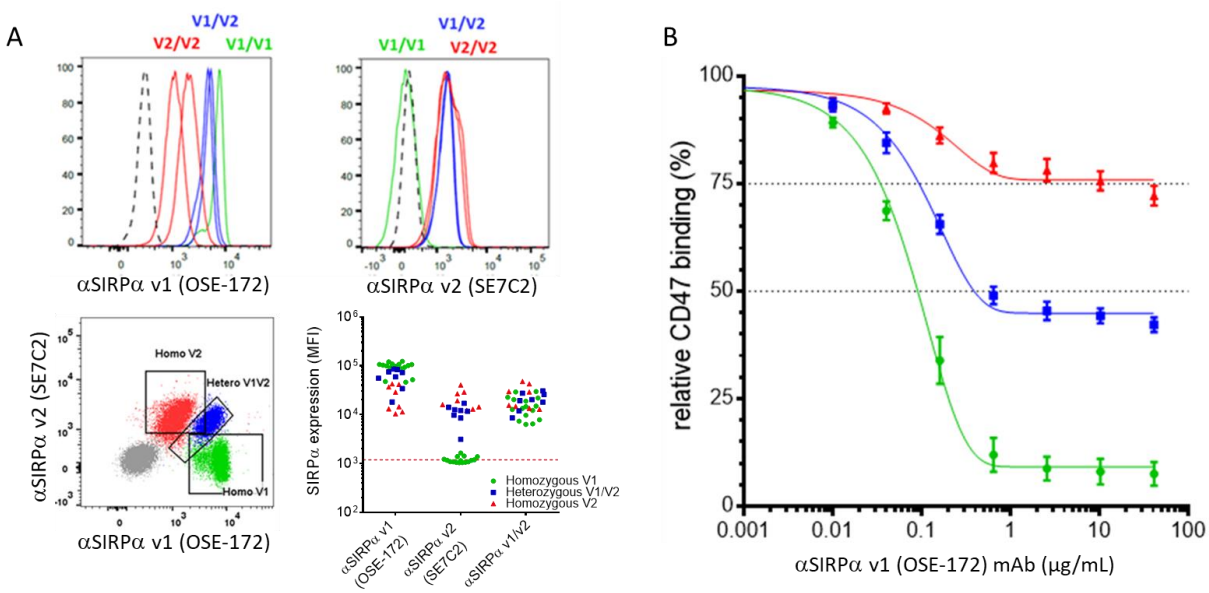

Extended Figure 13: Selective anti-human SIRPα mAb (OSE-172) as compare to the anti-SIRPα and SIRPγ mAb (Kwar23) binding and antagonist property on SIRP family members

(**A**) Characterization of OSE-172 (red) and Kwar23 (blue) anti-SIRPα mAbs binding at different concentrations of mAbs on the three SIRP family members: SIRPα, SIRPβ, and SIRPγ by ELISA. (**B**) Antagonist ELISA assay with increasing mAb concentrations on SIRPα or SIRPγ immobilized to plastic, revealed by human CD47-hFc binding. (**C**) Competition assay of OSE-172 with Kwar23 or OSE-172 anti-SIRPα mAb on immobilized SIRPα by ELISA.

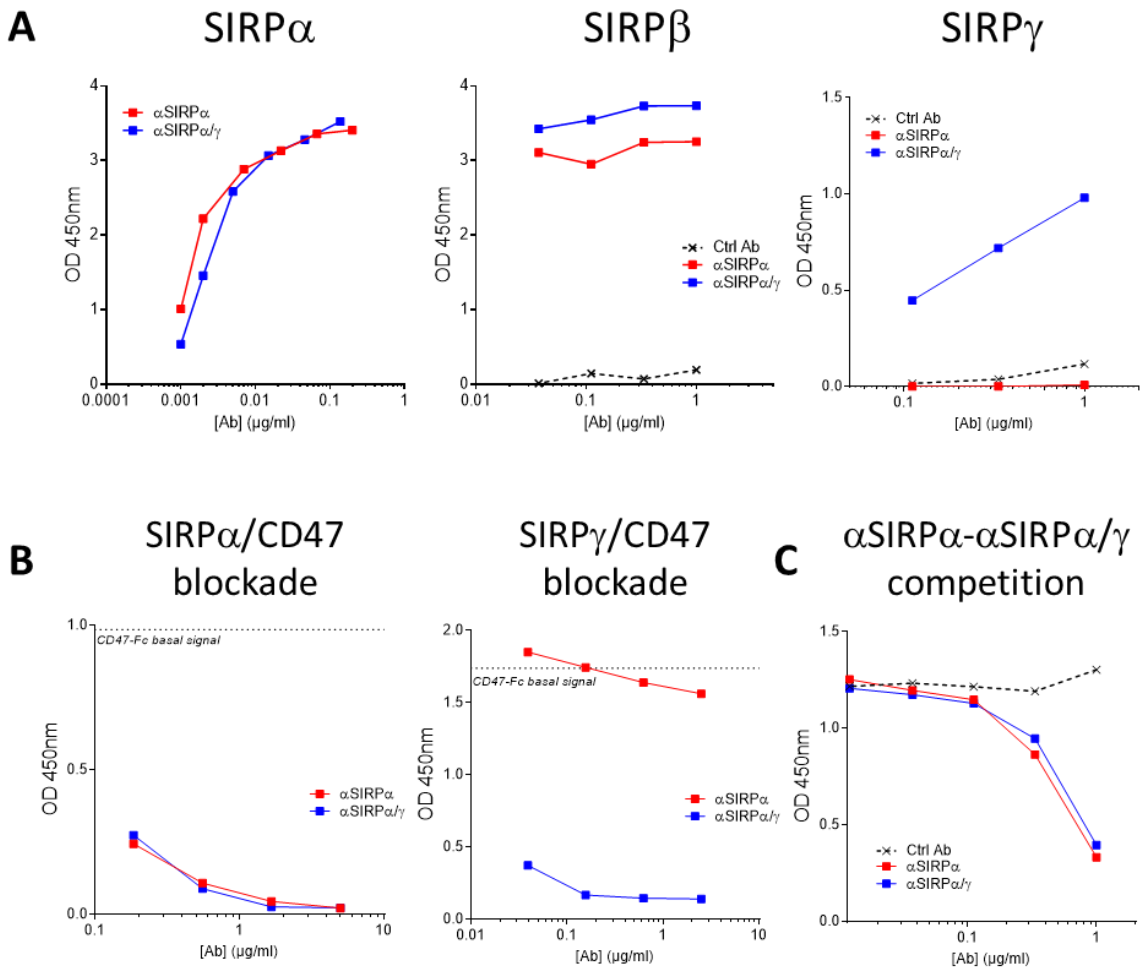

Extended Figure 14: Anti-human SIRPα mAbs binding on peripheral immune cells

Characterization of OSE-172 (red) and Kwar23 (blue) anti-SIRPα mAbs binding on the major blood immune cell populations by flow cytometry. *Top*: percentage of positive cells. *Bottom*: Median Fluorescence Intensity (MFI). Binding of OSE-172 and Kwar23 was evaluated on monocytes (CD14+), T cells (CD3+), B cells (CD19+), and GM-CSF induced MΦ, and compared to the binding of an anti-SIRPα/β mAb (SE5A5), a selective anti-SIRPβ mAb (B4B6), a selective anti-SIRPγ mAb (LSB2.20) and an anti-CD47 mAb (B6H12).

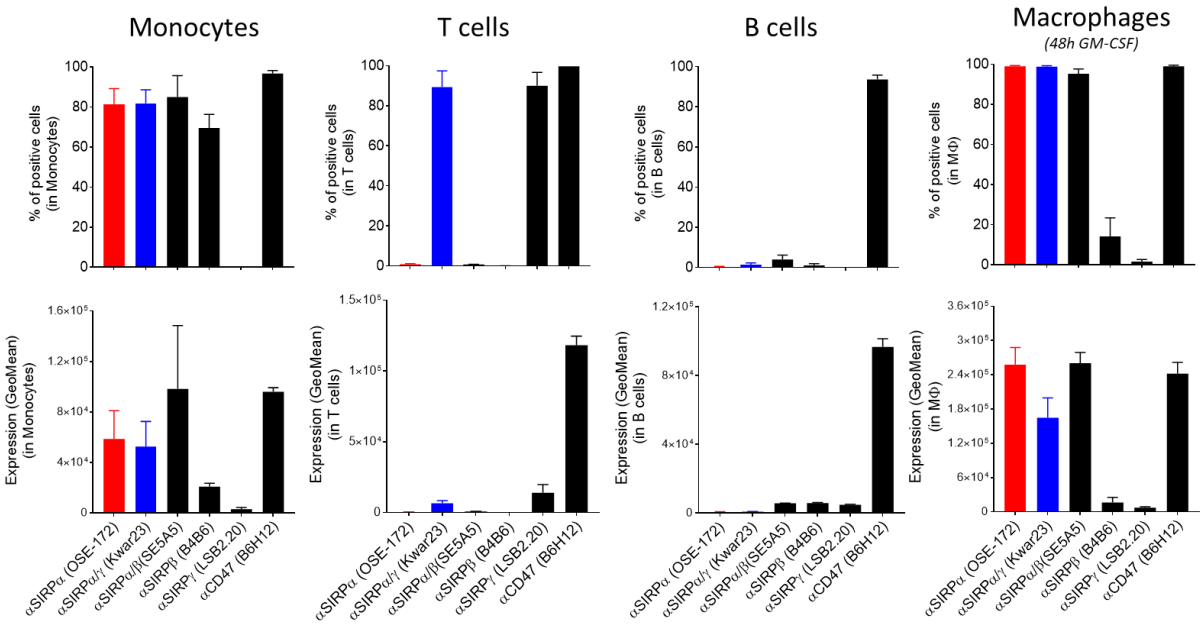

Extended Figure 15: SIRPα blockade by anti-human SIRPα mAbs (OSE-172 and Kwar23) increases phagocytosis of tumor cells

(**A**) 2h-Phagocytosis assay of CD47-hFc coated beads (red) compared to naked beads (blue) by human monocyte-derived dendritic cells preincubated with anti-SIRPα mAbs (OSE-172 or Kwar23) revealed by flow cytometry. (**B**) Phagocytosis assay of anti-CD20 (Rituximab)-opsonized Raji tumor cells (red) by M-CSF-derived Macrophages (green) for 2 hours in presence of anti-SIRPα mAbs (OSE-172 or Kwar23) and compared to the anti-CD47 (B6H12) revealed by microscopy. Pictures with phagocytosis events indicated by white arrows and fold increase of phagocytosis normalized to the control Ab for each donor are represented. **P* < 0.05, ***P* < 0.01 (unpaired Mann-Withney)

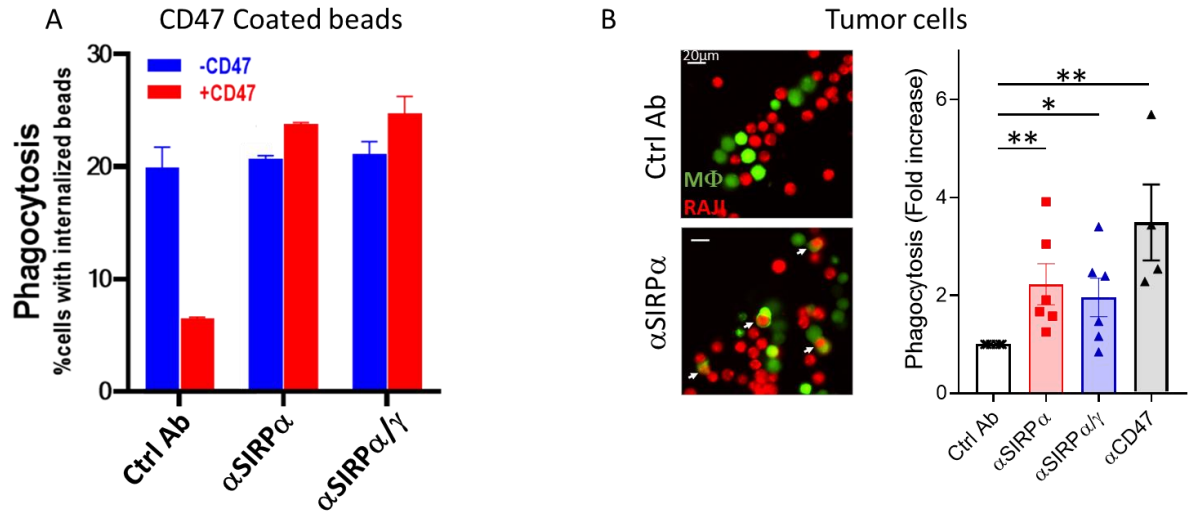

Extended Figure 16: List of significantly downregulated and upregulated gene expression after anti-SIRPα treatment of human tumor organoids

Downregulated	Upregulated	
CD46	HAVCR2	CREBBP
DOCK9	FCGR1A	IL17RA
HLA-A	KLRF1	F13A1
CD164	IFNA2	CR1
ST6GAL1	TMEFF2	VEGFC
HLA-C	BST1	IL11RA
PSMB7	TNFRSF17	TPTE
MAPK3	CCR2	CD38
ITCH	SLAMF6	IL26
MAP3K1	CCL1	IL2RB
MAP2K2	AXL	CD80
HLA-E	IL1RAPL2	SPO11
APP	JAM3	NLRP3
CD59	CD27	GZMA
CD47	XCL2	TNFSF4
ATF2	CXCR2	IL21
C4BPA	COLEC12	TARP
IL32	CLEC7A	TRAF3
	FUT5	CCL17
	CD8B	

Extended Figure 17: SIRPα and CD47 expression by human tumor cell lines

Flow cytometry phenotype of A549, Huh7, U373, U2OS, HeLa human tumor cell lines.

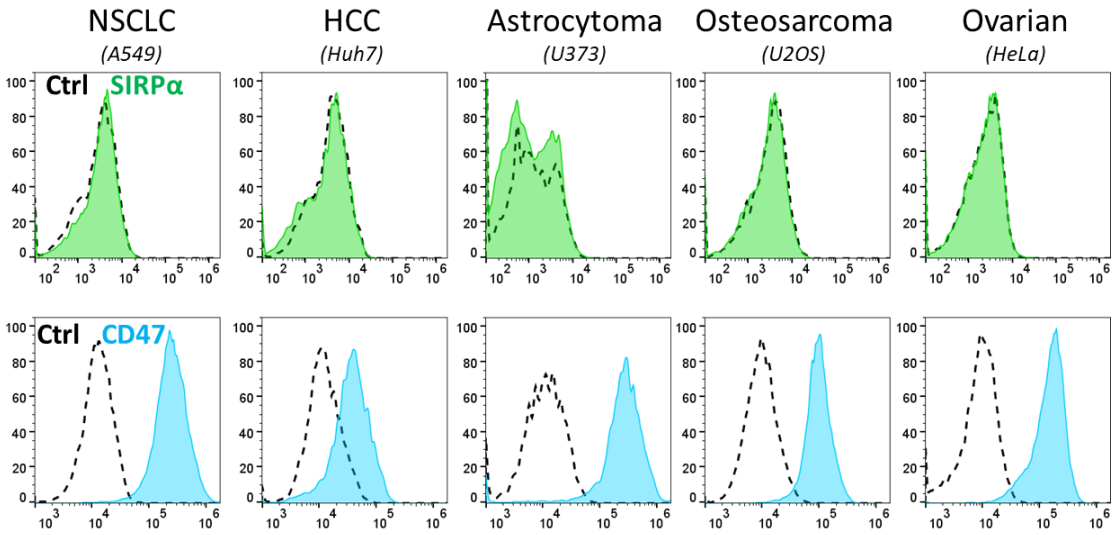

Extended Figure 18: Selective anti-SIRPα (OSE-172) and the anti-SIRPα/γ (Kwar23) mAbs enhance chemokine secretion by human macrophages

(**A**) CCL-3 chemokine secretion of human macrophages cultured for 24 hours on CD47-coated plastic with different mAb concentrations of an irrelevant control antibody, the selective anti-SIRPα (OSE-172), or the anti-SIRPα/γ mAbs (Kwar23). (**B**) CCL-4 chemokine secretion of human macrophages in the supernatant of spheroids cultured with 10µg/mL of the anti-SIRPα mAbs (OSE-172 or Kwar23). **P < 0.01 (paired Mann-Withney)

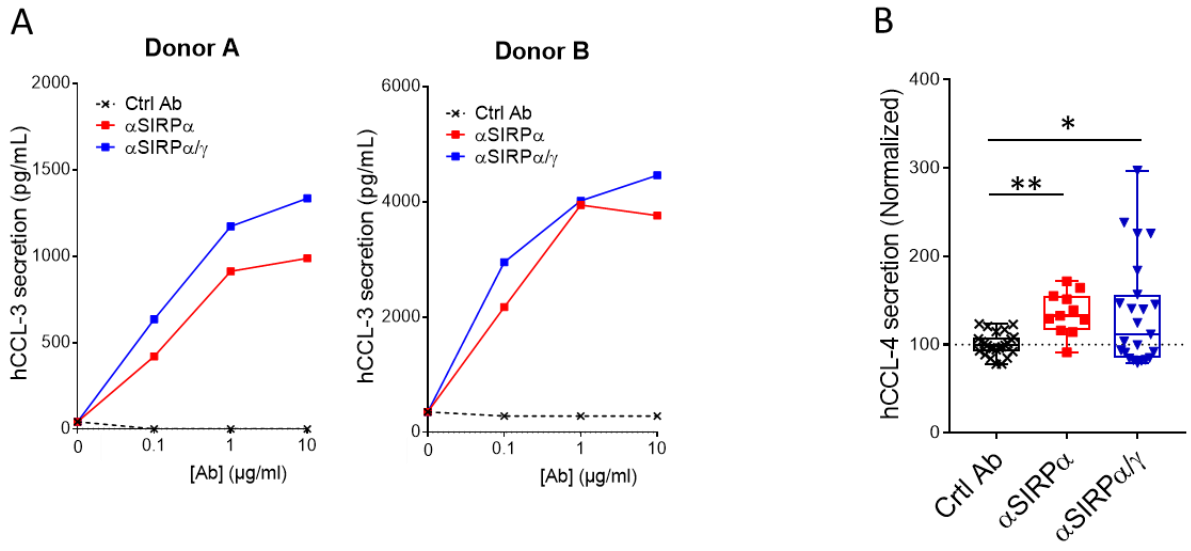

Extended Figure 19: Anti-SIRPα mAbs increases antigen-specific cross-presentation by mouse dendritic cells

(**A**) SIRPα expression by myeloid cell subsets was evaluated by flow cytometry on $CD11b^{-}$ $CD8\alpha^{+}$ cDC1 (blue), $CD11b^{+}CD8\alpha^{-}$ cDC2 (green) or $CD11b^{+}CD11c^{-}$ macrophages (black) as positive control. The dotted line represents the staining with isotype control. (**B**) Splenic cDC were isolated by flow cytometry cell sorting from C57Bl/6 WT mice and loaded with ovalbumin protein (OVA) at 100µg/mL overnight, then cultured with OVA specific-CD8 OT-I T cells at a 1:1 ratio for two days. OT-1 proliferation was assessed by H^3-thymidine incorporation. (**C**) cDC were loaded with OVA and cultured with OT-I cells as in (B) with anti-SIRPα mAbs or anti-CD47 at 10µg/mL. (**D-F**) C57Bl/6 mice were injected with anti-SIRPα MY1-mG1 mAb or an isotype control at 10mg/kg three times (d-1, d+1, d+3) and with 2.10^6 of CPDe450 stained OT-I T-cells at d0. OVA was injected i.p. (40µg/mouse) at day+1 and the spleen was collected at day+4 for flow cytometry analysis of DC phenotype with MHC-I, CD86, and CD103 markers (D) and OT-I T-cell proliferation (E-F). (E) Proliferation histograms of each mice according to the treatment were concatenated using FlowJo. (F) Proliferation index of OT-I T-cell proliferation was calculated using FlowJo (N=8/group). **P* < 0.05, ***P* < 0.01 (unpaired Mann-Withney or Kruskall-Wallis)

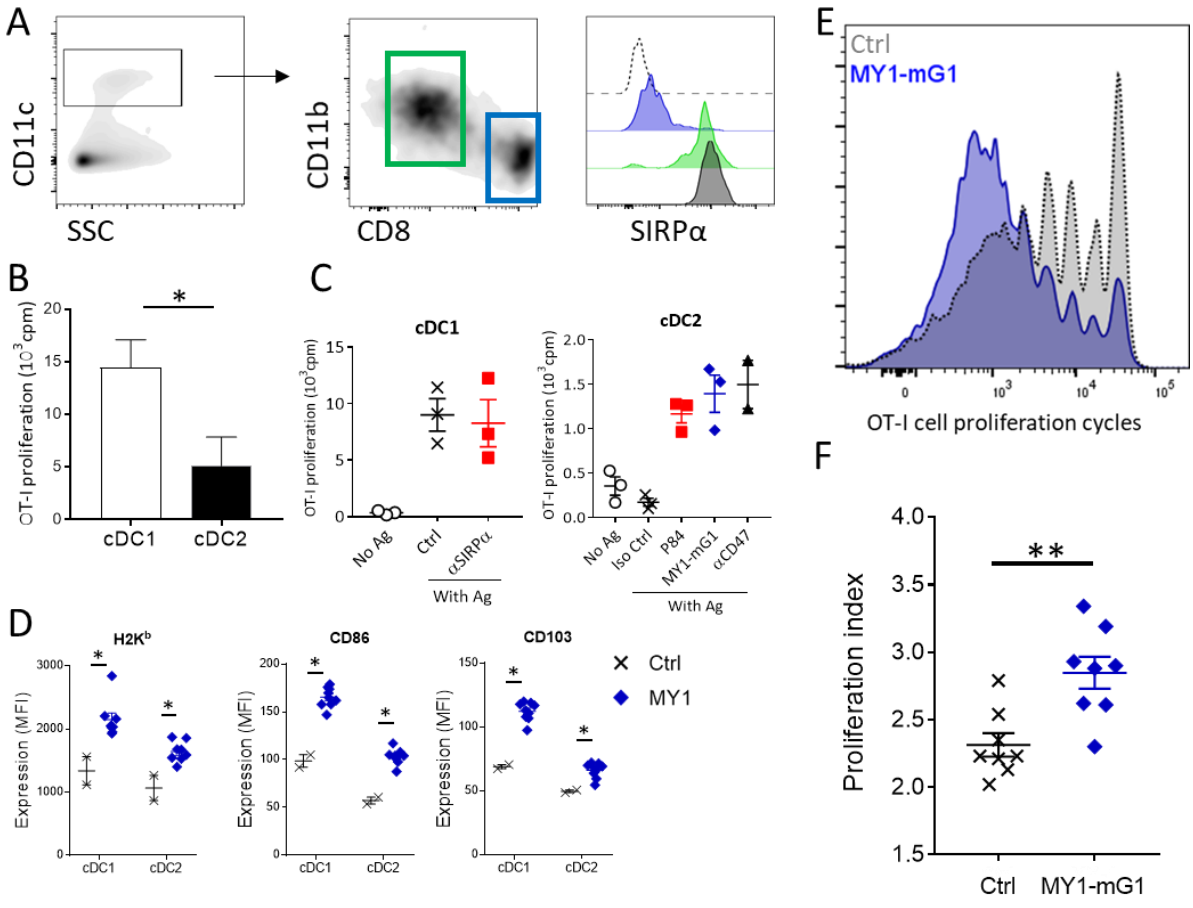

Extended Figure 20: SIRP family members scRNA-seq analysis in human PBMC

CD47, SIRPα, SIRPβ, SIRPγ RNA expression visualized in the single cell RNAseq dataset of Human PBMC of healthy volunteers (Ding *et al*, BioRxiv 2019) with the Broad Institute Single Cell portal (https://singlecell.broadinstitute.org/single_cell/study/SCP424/single-cell-comparison-pbmc-data#study-visualize)

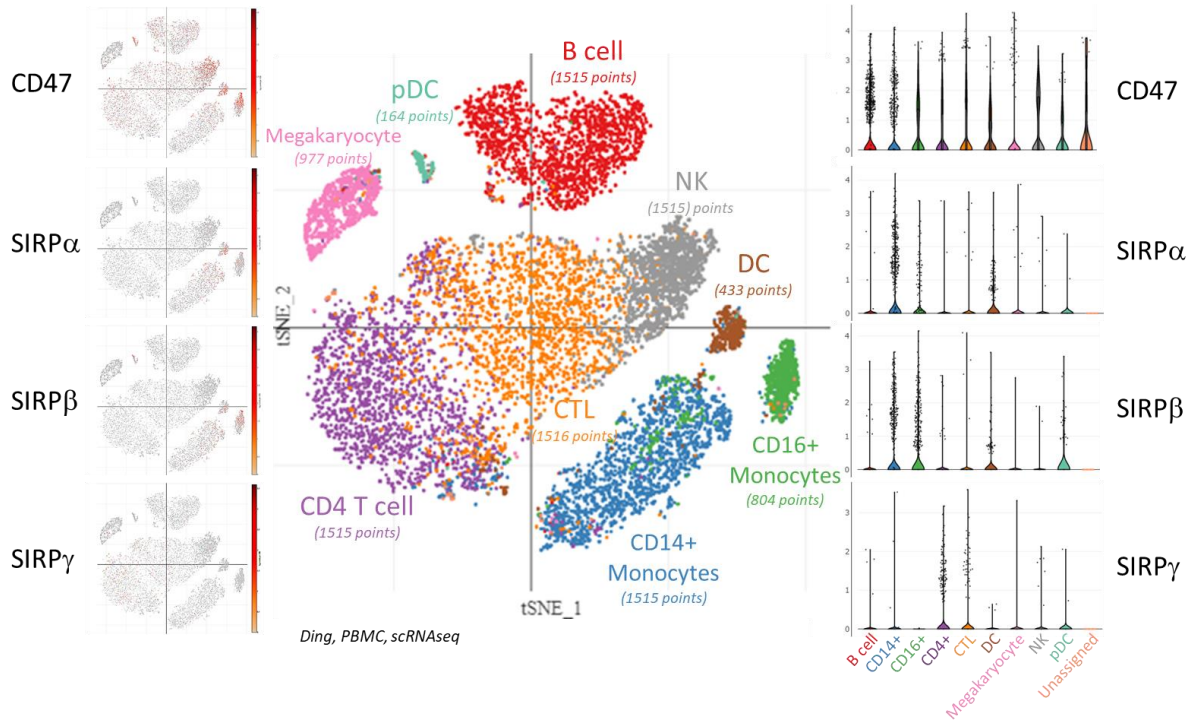

Extended Figure 21: SIRP family members scRNA-seq analysis in melanoma TILs

CD47, SIRPα, SIRPβ, SIRPγ RNA expression visualized in the single cell RNAseq dataset of Human TILs of melanoma patients (Jerby-Arnon *et al*, Cell 2018) with the Broad Institute Single Cell portal (https://singlecell.broadinstitute.org/single_cell/study/SCP109/melanoma-immunotherapy-resistance#study-visualize)

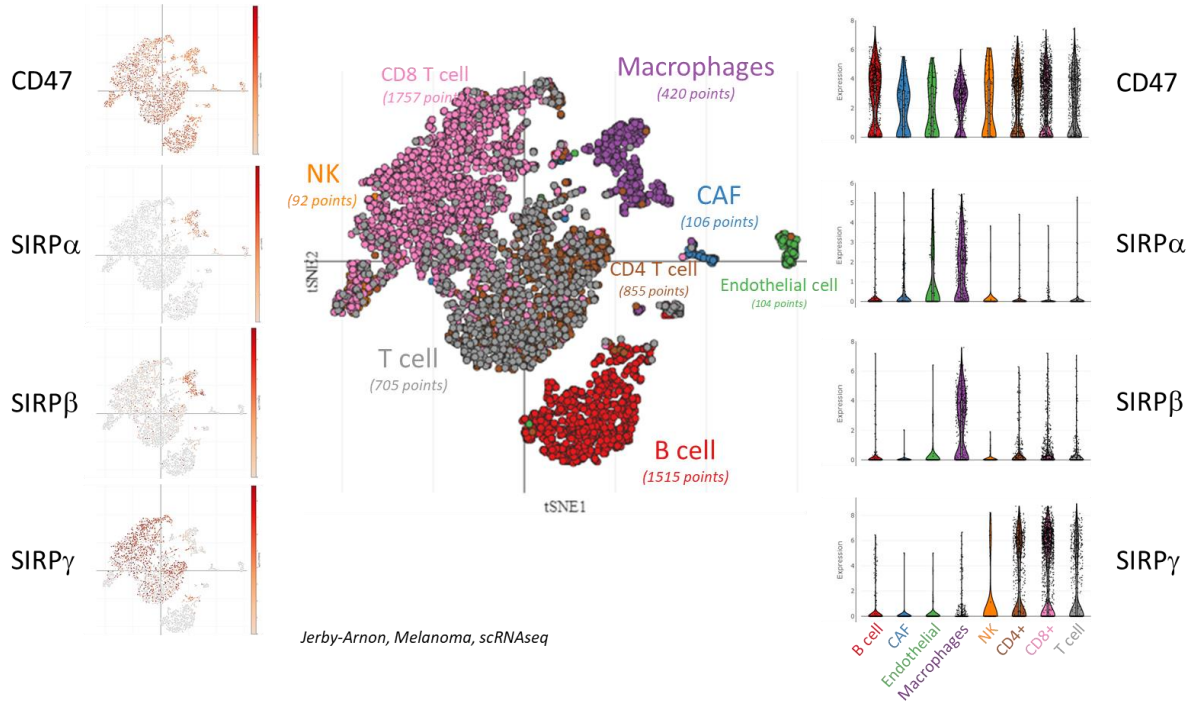

Extended Figure 22: SIRP family members scRNA-seq analysis in Human NSCLC TILs

CD47, SIRPα, SIRPβ, SIRPγ RNA expression visualized in the single cell RNAseq dataset (GSE127465) of Human TILs of NSCLC patients (Zilionis *et al*, Immunity 2019) with the Broad Institute Single Cell portal (https://singlecell.broadinstitute.org/single_cell/study/SCP739/single-cell-transcriptomics-of-human-and-mouse-lung-cancers-reveals-conserved-myeloid-populations-across-individuals-and-species#study-visualize)

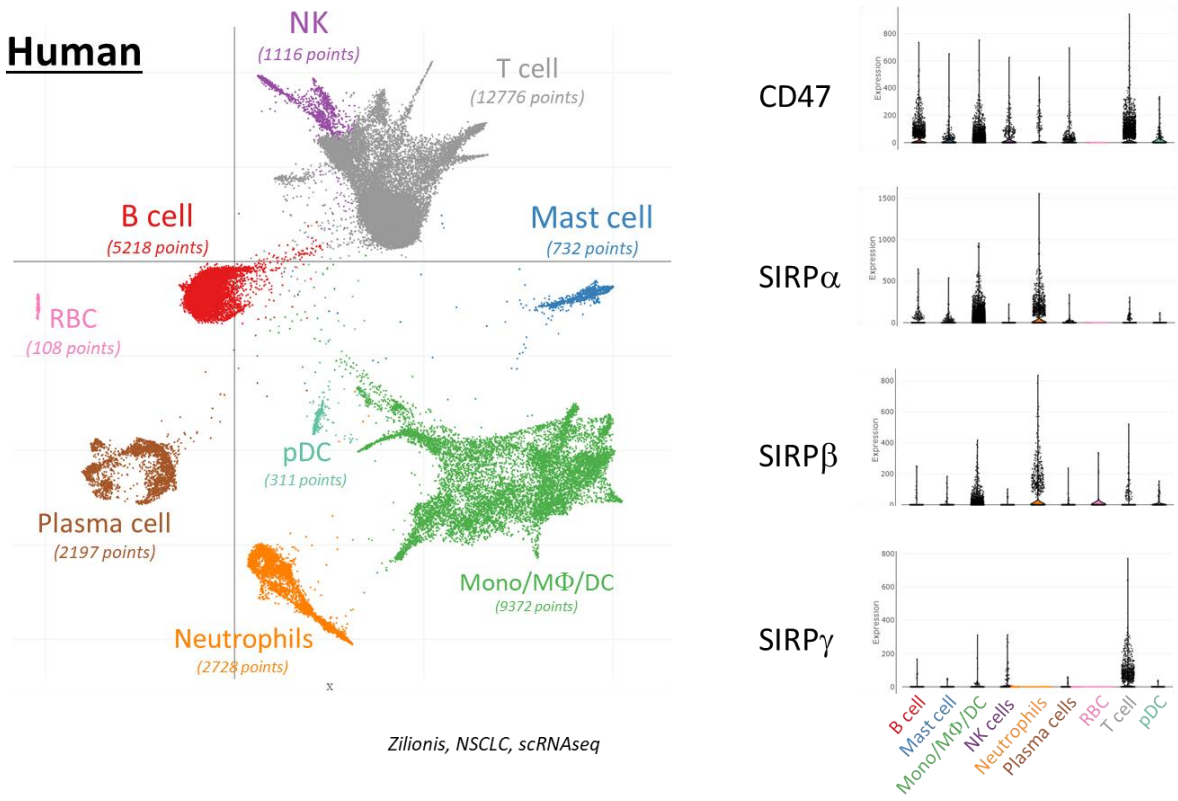

Extended Figure 23: SIRP family members scRNA-seq analysis in Mouse NSCLC TILs

CD47, SIRPα, SIRPβ, SIRPγ RNA expression visualized in the single cell RNAseq dataset (GSE127465) of Murine TILs of NSCLC patients (Zilionis *et al*, Immunity 2019) with the Broad Institute Single Cell portal (https://singlecell.broadinstitute.org/single_cell/study/SCP739/single-cell-transcriptomics-of-human-and-mouse-lung-cancers-reveals-conserved-myeloid-populations-across-individuals-and-species#study-visualize)

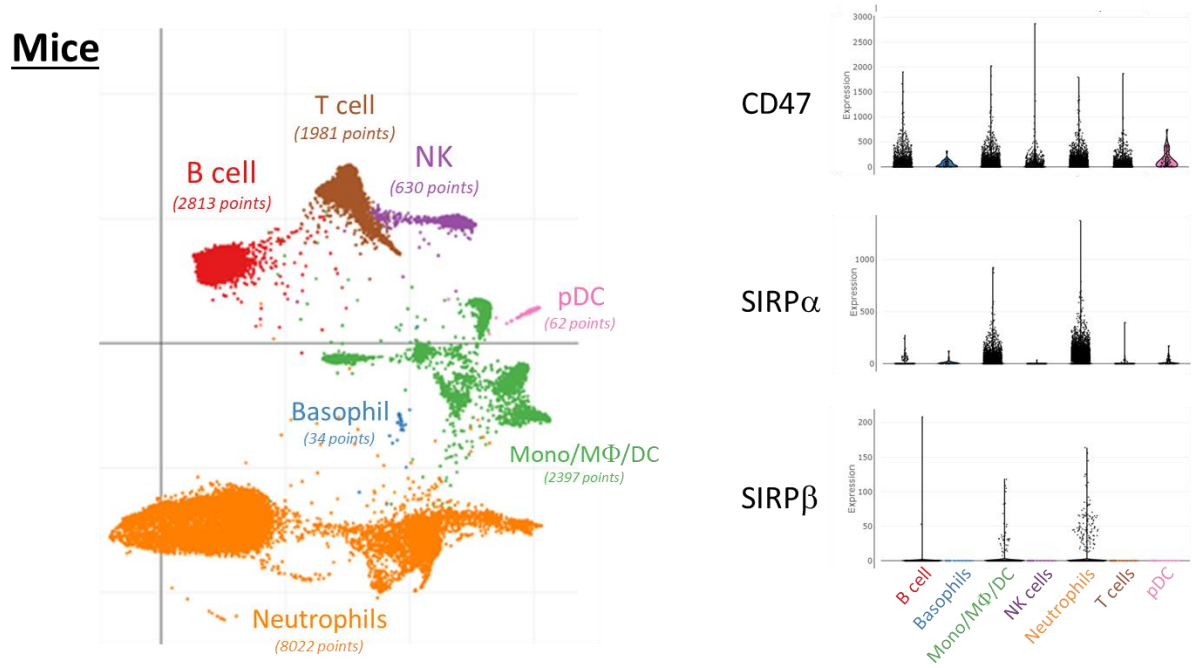

Zilionis, NSCLC, scRNAseq

Extended Figure 24: Phylogenetic tree of SIRP genes family members

Refseq protein sequences were extracted from NCBI in fasta format. Sequence alignment and phylogenetic tree was performed using clustal-O (ebi.ac.uk/Tools/msa/clustalo).

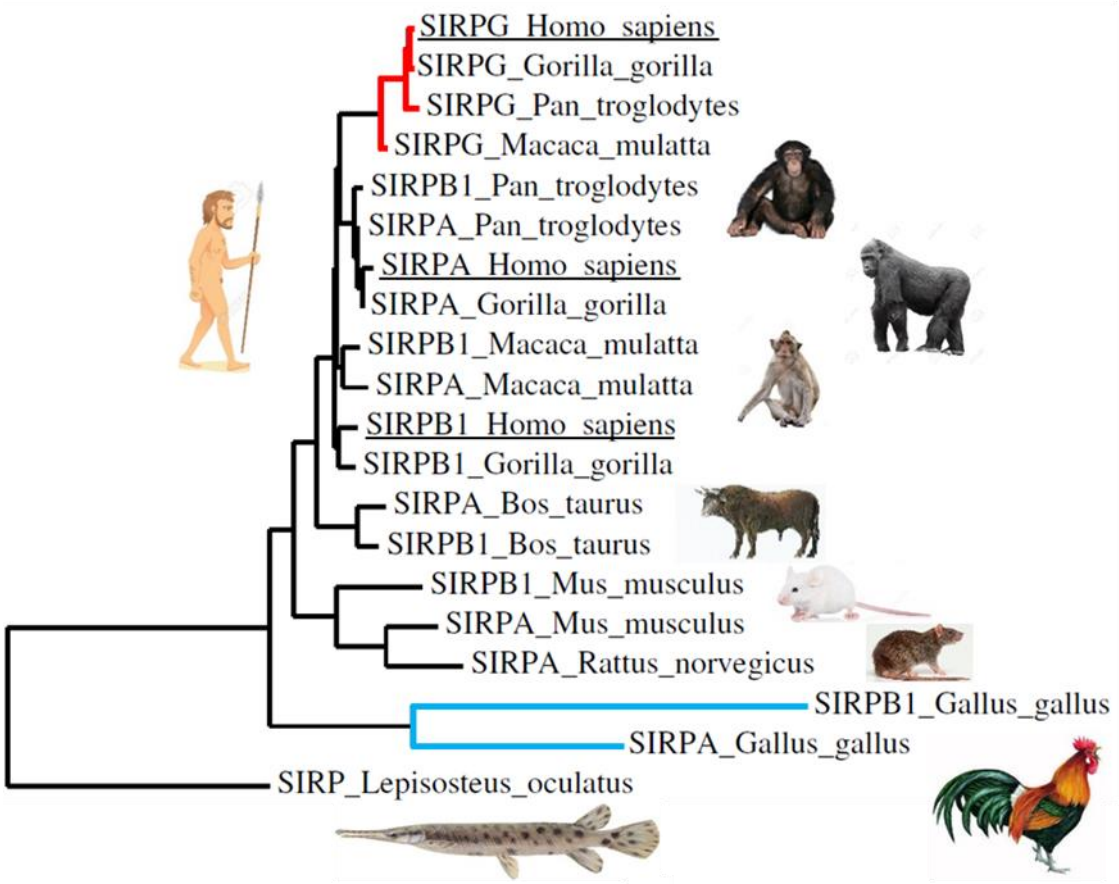

Supplemental methods

SIRP family members binding and antagonist assays by ELISA

SIRPα (0.5µg/mL), SIRPβ (1µg/mL), or SIRPγ (1µg/mL) were coated overnight in 96-well maxisorp plates in PBS buffer, then the anti-SIRPα mAbs (OSE-172 & Kwar23) were incubated 2h at 37°C at different concentrations and revealed with a HRP-coupled anti-hIgG Fc mAb. Antagonist assay was performed by adding CD47-Fc recombinant protein (6µg/mL) simultaneously to the anti-SIRPα mAbs (OSE-172 & Kwar23) and revealed by a HRP-coupled streptavidin (0.2µg/mL).

SIRP family members binding and antagonist assays by Flow cytometry

Tumor cell lines or frozen human monocytes are thawed, died cells labelled with LIVE/DEAD Fixable Yellow Dead cell stain kit, Fc receptors are blocked with human FcBlock reagent in presence of human serum and then labelled 30min on ice with anti-SIRPα mAb (OSE-172), anti-SIRPα/γ mAbs (Kwar23), anti-SIRPα mAb (SE7C2), anti-SIRPα/β mAb (SE5A5) anti-SIRPβ mAb (B4B6) anti-SIRPγ mAb (LSB2.20), or anti-CD47 (B6H12) at 10µg/mL or at different concentrations when it is mentioned, and then revealed with a PE-coupled anti-hIgG Fc or anti-mIgG1 mAbs. For PBMC analysis, anti-CD3 (SK3), -CD14 (M5E2), -CD19 (APC), were added to identify T-cell, monocytes and B-cell respectively. Antagonist assay was performed by adding CD47-Fc recombinant protein (10µg/mL) simultaneously to the anti-SIRPα mAbs (OSE-172 & Kwar23) and revealed by a PE-coupled streptavidin.

Time-lapse & CD47 coated-beads phagocytosis evaluation

Phagocytosis by macrophages: M0 macrophages were harvested by TryPLE express (GIBCO) digestion and gentle scrapping after 5 to 6 days differentiation. The cells were counted and stained with 1µM Calcein-AM (TOCRIS) in serum free RPMI medium for 30 min at 37°C at a concentration of 106 cells / ml. The cells were then centrifuged and resuspended in complete medium containing the indicated antibodies and split into IBIDI chambers precoated with 10µg/ml of Poly-Lysine (Sigma Aldrich) and put back at 37°C and 5% CO2 for 1 hour. RAJI cells were counted and stained as the macrophages, except with 1.5µM CellTracker™ Deep Red Dye (Molecular Probes). The cells were then then centrifuged and resuspended in complete

medium containing Rituximab +/- B6H12 and put back at 37°C and 5% CO2 for 15 minutes. Opsonised RAJI cells were then added to the settled macrophages at a ratio of 2:1. The final concentration of antibodies was 10µg/ml except Rituximab (1 to 10 ng/ml). The phagocytosis was imaged on a Nikon Ti2E microscope were cells were kept at 37°c and 5% CO2 all through the imaging process, that started 20 minutes after cell contact, for up to 2 hours. Pictures were taken every 5 to 10 minutes through a PLAN APO LBDA 20X 0,75/1 mm objective. The percentage of phagocytosis was assessed on the 2 hours time span, on at least 400 macrophages, and calculated as : (number of phagocyting macrophages/ total macrophages) x 100. The results are expressed as percentage of the phagocytosis fold change normalized with the control condition.

Phagocytosis by human dendritic cells: human monocyte-derived dendritic cells were prepared from donors confirmed as V1-homozygous by genotyping. Dendritic cells were preincubated with anti-SIRPα antibodies at a concentration of 10 µg/mL for 30 minutes. Streptavidin-coated, pacific blue-labeled microbeads (3.0 µM diameter, Spherotec), were bound to biotinylated human CD47 (coated at RT for 30 min, 12 µg/ml) washed, and then opsonized with human IgG1 antibodies to induce Fc-receptor mediated phagocytosis. Beads were added at a ratio of 20:1 to dendritic cells pre-treated with SIRPα antagonists or isotype control antibodies. After 2 hours at 37C, cells were harvested and analyzed by flow cytometry to quantify the number of cells that had fully internalized beads.

Single cell RNAseq visualisation

The single cell RNAseq datas generated in the three papers are available on the Single Cell Portal with the links referenced below :

- Ding J on human PBMC: https://singlecell.broadinstitute.org/single_cell/study/SCP424/single-cell-comparison-pbmc-data#study-visualize
- Jerby-Arnon L on Immune Checkpoint Inhibitors (ICI) melanoma cells : https://singlecell.broadinstitute.org/single_cell/study/SCP109/melanoma-immunotherapy-resistance#study-visualize
- Zilionis R on Tumor-infiltrating Myeloid cells (TIMs) from human and mouse lung cancers (GSE127465): https://singlecell.broadinstitute.org/single_cell/study/SCP739/single-cell-

transcriptomics-of-human-and-mouse-lung-cancers-reveals-conserved-myeloid-populations-across-individuals-and-species#study-visualize